LAWRENCE
LIVERMORE
NATIONAL
LABORATORY

UCRL-CONF-201209

ALE3D Model Predictions and Experimental Analysis of the Cookoff Response of Comp B*

M. A. McClelland, J. L. Maienschein, J. E. Reaugh, T. D. Tran, A. L. Nichols, J. F. Wardell

December 1, 2003

Joint Army Navy NASA Air Force (JANNAF) Meeting
Colorado Springs, CO, United States
December 1, 2003 through December 5, 2003

ALE3D Model Predictions and Experimental Analysis of the Cookoff Response of Comp B*

M. A. McClelland, J. L. Maienschein, J. E. Reaugh, T. D. Tran,
A. L. Nichols, and J. F. Wardell
Lawrence Livermore National Laboratory

ABSTRACT

ALE3D simulations are presented for the thermal explosion of Comp B (RDX,TNT) in a Scaled Thermal Explosion Experiment (STEX). Candidate models and numerical strategies are being tested using the ALE3D code which simulates the coupled thermal, mechanical, and chemical behavior during heating, ignition, and explosion. The mechanical behavior of the solid constituents is represented by a Steinberg-Guinan model while polynomial and gamma-law expressions are used for the equation of state of the solid and gas species, respectively. A gamma-law model is employed for the air in gaps, and a mixed material model is used for the interface between air and explosive. A three-step chemical kinetics model is used for each of the RDX and TNT reaction sequences during the heating and ignition phases, and a pressure-dependent deflagration model is employed during the rapid expansion. Parameters for the three-step kinetics model are specified using measurements of the One-Dimensional-Time-to-Explosion (ODTX), while measurements for burn rate are employed to determine parameters in the burn front model. We compare model predictions to measurements for temperature fields, ignition temperature, and tube wall strain during the heating, ignition, and explosive phases.

INTRODUCTION

Computational tools are being developed to predict the response of munitions and propellant systems to abnormal thermal (cookoff) events. Lawrence Livermore National Laboratory[1,2] (LLNL), Sandia National Laboratory[3] (SNL), the Naval Air Warfare Center[4] (NAWC) are performing cookoff experiments to improve DOE computer codes and associated thermal, chemical, and mechanical models. Cookoff behavior has been investigated for a number of explosives in the STEX system shown in Figure 1. A sealed tube with heavily reinforced ends is heated slowly until ignition occurs. The response is characterized using thermocouples, strain gauges, and a radar system to measure fragment velocities. The design of this cookoff system is relatively simple to facilitate model and code development. An effort is being made to achieve a wide range of results for reaction violence.

We are developing computer codes and materials models to simulate cookoff for ordnance safety evaluations. The computer program ALE3D from LLNL is being used to simulate the coupled thermal transport, chemical reactions, and mechanical response during heating and explosion[5, 6]. SNL is employing multiple computer codes in a parallel effort[7]. Atwood et al.[8] measured mechanical, physical, and chemical properties of PBXN-109, and Erikson et al.[9] performed thermal, chemical, and mechanical simulations of the NAWC tests. Their predicted cookoff temperatures were generally in good agreement with values measured in several NAWC tests[10]. They also presented initial calculations showing the expansion of the containment tube after ignition which were refined in a later investigation[7, 11]. In an earlier paper[12] we discussed ALE3D models for cookoff of PBXN-109, and presented measurements for thermal expansion, heat capacity, shear modulus, bulk modulus, and ODTX. Later those measurements were used to determine model parameters, and ALE3D predictions for explosion temperature were in satisfactory agreement with NAWC measurements[6,13]. We provided initial ALE3D simulations for slow cookoff in which thermal, mechanical, and chemical behavior were modeled through the heating, ignition, and explosion phases. Although these initial strain results were only approximate, they helped to guide

* Approved for public release, distribution is unlimited. Work performed under the auspices of the U.S. Department of Energy by Lawrence Livermore National Laboratory under contract No. W-7405-ENG-48.

improvement in numerical strategies. Later Yoh and McClelland[14] gave more accurate results for mechanical behavior in STEX tests involving PBXN-109. Here we give initial ALE3D results for the cookoff of Comp B in the STEX system.

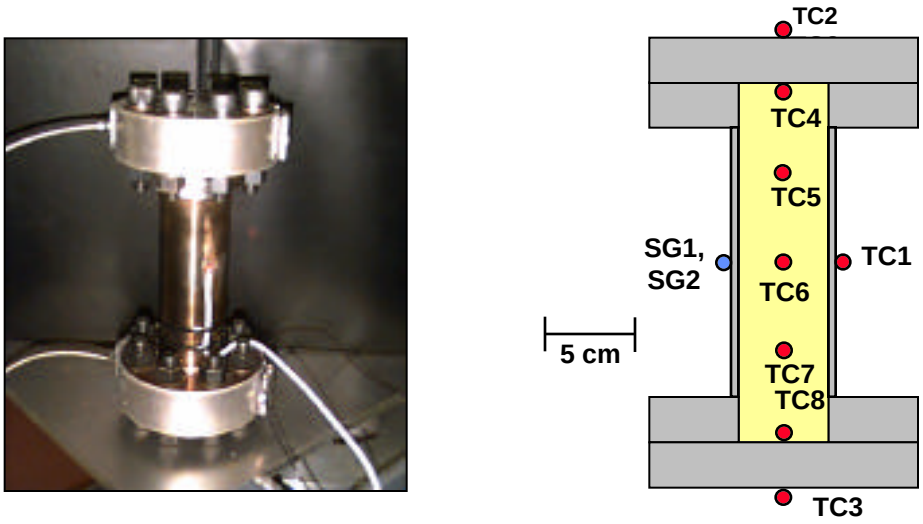

Figure 1 Schematic of geometry and instrumentation for STEX cookoff test TE-012 for Comp B.

SCALED THERMAL EXPLOSION EXPERIMENTS

Maienschein and Wardell[15, 16] performed a series of STEX tests with cylindrical charges of Comp B (64% RDX, 36% TNT, 1% wax) confined in a steel tube with sealed ends (see Figure 1). In each test, the vessel had an inside length of 20.32 cm and an inside diameter of 5.08 cm giving a nominal aspect ratio of L/D=4. For the selected test (TE-012) of this study, the 4130 steel tube has a 0.406 cm wall thickness, providing a confinement pressure of approximately 2 kbar (200 MPa). The end seals are achieved with O-rings bolted between flanges. In this test, 646 g of Comp B was introduced into the vessel as three cast sections leaving approximately 10% ullage, based on a nominal density of 1.75 g/cm^3. Three radiant heaters spaced at 120° provide the energy to heat the sides of the vessel while two independent resistance heaters are used to heat the top and bottom flanges of the assembly.

For each test, the temperature is measured at five internal locations (TC4-TC8) using a probe and many external locations on the outer tube surface using RTDs. Three Proportional-Integral-Derivative (PID) controllers are used to adjust the heater powers in the top, bottom, and set of three side heaters to keep respective thermocouples at top (TC2), bottom (TC3), and side (TC1) locations near their set-point values. Two hoop (SG1, SG2), and two axial strain gauges were used to measure the deformation of the tube near the axial midplane during the thermal ramp and explosion. Three radar systems were used to measure the velocity of fragments. In this experiment, the final ramp rate for the set-point temperature was 1^{o}C/h.

ALE3D MODEL

ALE3D chemical, mechanical, and thermal models are being developed to model the cookoff of Comp B. The model composition is taken to be 64% RDX and 36% TNT with the wax neglected. In this version of our model, a separate and non-interacting chemical reaction sequence is employed for each of RDX and TNT. Each sequence is taken to have four components with three reaction steps following the models developed by McGuire and Tarver[17] and Tran et al.[18] for RDX and pure TNT:

$$A \rightarrow B \qquad r_1 = Z_1 \exp(-E_1/RT)\rho_A \qquad (1)$$

$$B \rightarrow C \qquad r_2 = Z_2 \exp(-E_2/RT)\rho_B \qquad (2)$$

$$C \rightarrow D \qquad r_3 = Z_3 \exp(-E_3/RT)\rho_C^{\,n} \qquad (3)$$

Here ρ_i is the mass concentration of a reactant i. The quantities r_j, Z_j and E_j are the reaction rate, frequency factor and activation energy, respectively, for a reaction j. The value for the reaction order n in reaction (3) is 2 for RDX and 1 for TNT. For RDX, component A is solid RDX, component B is an intermediate with material properties assumed to be the same as component A, and components C and D are gases. For TNT, component A is liquid TNT, component B is an intermediate with the same material properties and components C and D are gases. The condensed phases for TNT are selected to be liquids since this is the phase of TNT (T_{mp}=81°C) present at the usual temperatures of slow cookoff for Comp B. A more complete model is in development to include the solid phase of TNT as an additional TNT species. A kinetics melting model will be employed to transition from the solid to liquid TNT species[19]. In the next section model predictions are compared with measured values for the ODTX.

After the Arrhenius reaction rates have increased to the point where changes are occurring on a time scale the time scale of sound propagation, a switch is made to a burn front model in which reactants are converted to products in a single reaction step. This switch in models is made for two reasons. The first is that the computational capabilities and methods are not yet available to resolve reaction zones which can be on the scale of nanometers. The second reason is that Arrhenius kinetics measured on the time scale of 1-10^4 s in the ODTX apparatus may not apply on shorter time scales. It is likely that deflagration rates measured in the strand burner described below provide a better measure of reaction behavior on short time scales. We assume that the burn front velocity, V, is a function of the pressure, P, at the front location, and use power-law expressions of the form:

$$V = V_0(p/p_0)^n \qquad (4)$$

Here the subscript 0 indicates a reference quantity. The selection of parameters for Comp B is discussed below in the section on burn rates.

The mechanical models for the condensed HE constituents along with the steel components are taken to have Steinberg-Guinan[20] mechanical models. The shear modulus and yield stress are taken to be zero for the liquid components of TNT (TNTA and TNTB). The shear modulus and yield stress are also taken to be zero for the Comp B mixture since the mixture is 36% liquid TNT in the cookoff temperature range of interest. A more detailed model would incorporate the viscous effects from the liquid TNT and the elastic contribution of the matrix of RDX particles. It is also noted that the Steinberg-Guinan model for 4340 steel is used for the 4130 steel.

A 7-term polynomial expression is used for the equations of state for the condensed RDX and TNT components. The constant volume heat capacity does not vary with temperature in this EOS. Calculated melt and cold curves are used to account for the influence of compression on melting energy. A nonlinear regression[13] procedure was used to determine the coefficients that give an optimum representation of the measurements of CTE, hydrostatic compression, and the unreacted shock Hugoniot The liquid TNT models were developed to match behavior for the liquid above the melting point and were extrapolated below the melting point to room temperature. Since the Comp B mixture is composed of a solid matrix of RDX particles and TNT liquid, these models are expected to provide only an approximate description of actual behavior.

The model gas constituents (C, D) for RDX and TNT along with the air in the gap are treated as no-strength materials with gamma-law equations of state. This equation of state provides an approximate representation over much of the pressure range, except at the higher pressures of 10 kbar (1 GPa) where the model may be less accurate. The Γ-value for the HE gas species is set using a pressure of 1 kbar (100 MPa), a temperature of 2273°K, and the density and heat capacity from the thermo-chemical equilibrium computer code, CHEETAH 2.0[21] for the final product gases.

The time-dependent thermal transport model includes the effects of conduction, reaction, advection, and compression. The constant-volume heat capacity is constant for each reactant consistent with the Steinberg-Guinan model. The thermal conductivity for the condensed species A and B is taken

to be constant, whereas the effects of temperature are included for the gaseous species. The heat capacity for gases C and D is assigned the same constant-volume value used in the gamma-law model. The temperature-dependent thermal conductivity is estimated at 1 kbar (100 MPa) using Bridgman's[22] equation for liquids in which the sound velocity is calculated using results from CHEETAH.

CHEMICAL KINETICS MEASUREMENTS AND MODEL REPRESENTATION

One-Dimensional-Time-to-Explosion (ODTX)

ODTX measurements were made for Comp B using the standard apparatus at LLNL[18, 23] (see Figure 2). In this system, the outer surface temperature of a 1.27 cm diameter sphere of HE is suddenly increased to a higher set-point temperature. The time to explosion is the time elapsed from the start of heating until confinement failure. The measurements of this study along with previous measurements are plotted as a function of temperature in Figure 2.

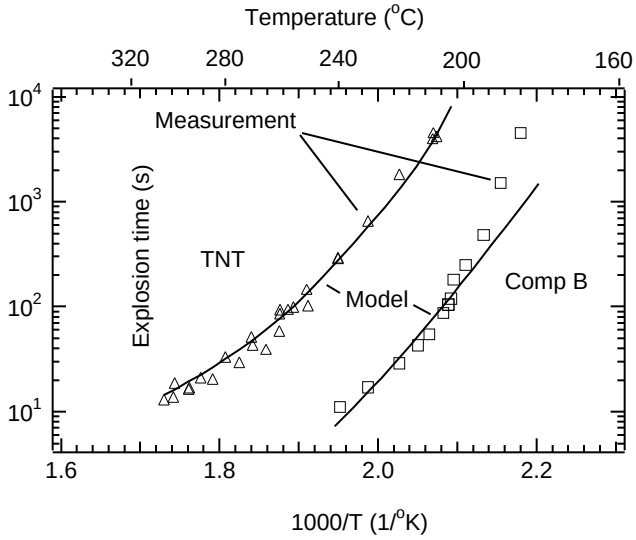

Figure 2 Comparison of measured and model ODTX results for Comp B and TNT.

Calculated explosion times for Comp B are also shown in Figure 2 for a one-dimensional model involving transient heat conduction and the two chemical reaction sequences[17,18] (Eqs. (1)-(3) for RDX and TNT). The model parameters were obtained in two steps. First parameters in a recent 3-step model for pure TNT were adjusted for use with ALE3D to represent the TNT ODTX data. Then kinetics parameters in the RDX component of the Comp B model (McGuire Tarver) were adjusted to represent the Comp B ODTX data. The latter adjustments were confined to the RDX model since RDX ignites at a lower temperature than TNT, and essentially determines the time to explosion. One-dimensional explosion times were calculated using TOPAZ2D[19, 24] and a mesh with 50 elements uniformly spaced in the radial direction. The TNT model provides a good representation of the ODTX data over the entire temperature range. The Comp B measurements are well represented above a temperatures of 196°C, but the model is less satisfactory below these temperatures.

Burn Rate Measurements for Comp B

The deflagration rate of Comp B was measured with the LLNL High Pressure Strand Burner[15,16]. This system measures pressure during the burn and also the progress of the burn front with wires that melt as the flame advances. Cylindrical samples 6.4 mm diameter x 5.7 cm long are prepared by stacking nine pieces to form a burn tower. Temporal pressure data along with time of arrival data at each burn wire provide the information to calculate burn rate as a function of pressure.

The deflagration rate measurements are plotted versus pressure in Figure 3 for samples burned at room temperature. It is seen that the burn rates are high and have considerable scatter. Below 10

MPa the measurements seem to follow a single curve, suggesting a smooth laminar burn. At higher pressures the data points vary by as much at two orders of magnitude. It is likely that the samples are deconsolidating which is possibly related to the melting of TNT. It is of interest to note that the lower bound of the data follows a curve with a second-order dependence which is high compared to other explosives. In later tests (not shown), deflagration measurements for Comp B at 100 °C were made to explore the effects of molten TNT. The measurements generally fall within the same band as the room temperature measurements. They show a weaker pressure dependence between 20 and 200 MPa, but seem to have the same strong dependence on burn rate above 200 MPa.

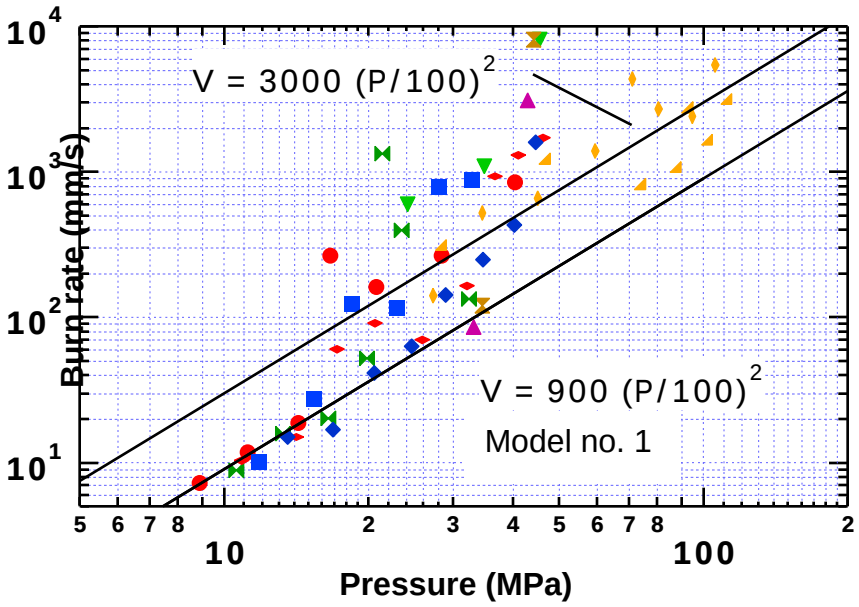

Figure 3. Model and deflagration rate data for Comp B. Each set of symbols represents data from one experiment.

Although we do not completely understand the physical phenomena associated with this burn rate data, we explore general trends using the burn-rate expression (4) in our ALE3D simulations. We use two burn rate curves with a second order dependence (see Figure 3). Model no. 1 is the lower bound for the measurements, and Model no. 2 curve passes through the middle of the data. It is an open and important question as to how to extrapolate the data since the model pressures for Comp B generally range from 100 to 1000 MPa. The pressure dependence of the burn velocity must become weaker at some point since the detonation velocity of Comp B is 8 km/s at 30 GPa[25]. Model calculations will help to reveal the sensitivity to these parameters.

BOUNDARY CONDITIONS AND NUMERICAL METHOD

Boundary Conditions

A two-dimensional, axisymmetric ALE3D model is used to simulate the cookoff of Comp B in cookoff Test TE-012. Boundary conditions for this model are shown schematically in Figure 4. The two-dimensional model includes 8% ullage on the HE ends and no ullage on the side. The 8% initial ullage is smaller than the10% physical value to be consistent with the use of a liquid TNT model over the entire temperature range. The gap is filled with air described by a gamma-law model in which the constant volume heat capacity is increased by a factor of 10 above its physical value to reduce spurious temperature increases associated with rapid compression. The HE and air do not slip at the wall, and all components of the vessel assembly are taken to be perfectly joined.

The top, bottom, and side heaters are applied as uniform heat flux conditions on the top, bottom, and side surfaces. Included among the side heater surfaces are the sides of the tube and flanges along

with the inward facing surfaces of the flanges. The heat fluxes for these three heaters are adjusted using three independent PI controllers to maintain the temperatures TC1, TC2, and TC3 at their set-point values (see Figures 1 and 4). The PI controller is tuned using the strategy of Internal Model Control[26] in which the steel regions are treated as a first-order lumped-capacitance systems with a single heat transfer coefficient to account for thermal losses to the surrounding air. Thermal convection is applied to all outward facing surfaces using heat transfer coefficients for laminar flow of air past appropriate model surfaces such as vertical and horizontal plates[27]. Standard expressions for hemispherical radiation are used on these same surfaces. A boundary layer expression for heat transfer resulting from the flow of air past a vertical plate is used on the tube surface. This expression has a dependence on the vertical coordinate, and is used to compensate for preferential cooling observed on the lower portion of the tube. In both the model and experiment, the top temperature TC2 is kept 5°C cooler than the lower temperature TC3 in an attempt to keep the ignition point near the axial midplane.

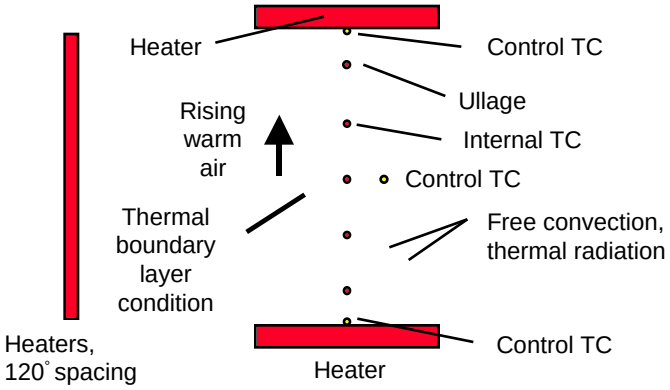

Figure 4 Boundary conditions for ALE3D axisymmetric model of STEX test for Comp B.

Meshes and Numerical Strategy

The ALE3D computer code requires 3D meshes, and a wedge-shaped mesh is employed for the 2D model of this study (see Figure 5). A small hole is present near the symmetry axis to allow the use of hexahedral elements at all locations. The tube cavity has 12 elements in the radial direction, 40 in the axial direction, and 1 element in the azimuthal direction. The tube wall has 3 zones across its thickness. This coarse mesh is used for these initial exploratory calculations, and is probably satisfactory for thermal-chemical results prior to ignition, but is not sufficiently refined for accurate strain calculations after ignition. Initially, the HE occupies the entire cavity in the radial direction and 92% of the cavity in the axial direction (see Figure 5). The remainder of the tube cavity is filled with air modeled as described above. Some of the elements have both HE and air, and standard mixing rules are employed to calculate the energy, heat capacity, thermal conductivity, shear modulus, and equation of state[28]. Since TNT is all liquid at the temperatures of slow cookoff, Comp B is a very soft material that undergoes large deformation while expanding in the cavity. The mesh is smoothed using a combination of Lagrange and Eulerian algorithms. Nodes initially on the interface between the cavity and the steel remain on these boundaries while nodes interior to the cavity are advected through the flowing HE and air.

A fully implicit method is used for the integration of the thermal transport equations during the thermal ramp and much of the subsequent ignition process. After the time step has decreased to within a factor of 10 of the value given by the Courant condition, a switch is made from implicit to explicit integration of the thermal transport equation. During the thermal ramp and subsequent ignition process, the hydrodynamic equations are integrated using an explicit method with the material densities increased by a large factor to make the calculations computationally feasible.

However, there is the question of selecting an appropriate scale factor. If the densities are increased too much, then the mechanical response will be sluggish, but if the densities are too low the calculations will be too lengthy. An analysis involving the Courant condition can be helpful in selecting

this factor. Numerical stability with an explicit scheme requires that the time step Δt be smaller than the time for sound to travel the smallest grid spacing:

$$\Delta t = Co\Delta x/v \tag{5}$$

Here v is the sound speed, Δx is the grid spacing, and Co is the Courant number. For the reduced sound speed v_s resulting from density scaling, we would like to specify the sound transmission time τ over a characteristic length L of the cookoff system:

$$\tau = L/v_s \tag{6}$$

If we write Eq. (5) for the reduced sound speed in Eq. (6) and combine the result with the original Eq. (5) the result for the mass scaled time step size is

$$\Delta t_s = \Delta t\, \tau\, v/L \tag{7}$$

in which $\tau\, v/L$ is the scale factor. Consider a Comp B cookoff experiment with a ramp rate 1°C/h, an HE length L of 20.32 cm, a sound speed v for TNT of 2 km/s, and a typical Courant time step size of $\Delta t = 3\times10^{-8}$ s. For a desired mechanical response time τ of 2 h (7200 s) which corresponds to 2°C of thermal expansion, Eq. (7) gives a mass-scaled time step size Δt_s of 2 s. Time steps of this size generate a large number of steps for a multi-day experiment, and more sophisticated procedures involving subcycling of the hydrodynamic integration are being developed to reduce computation time. Calculations of this type were used to establish the time step size Δt_s during the various phases of the thermal ramp. During the ignition process the value for Δt_s is set by the rate of chemical reaction and its associated error tolerances. Eventually the scale factor becomes unity and all equations are integrated explicitly with the densities at their physical values.

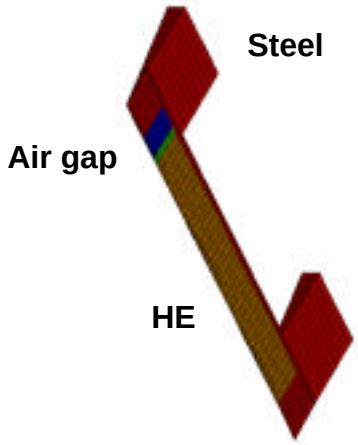

Figure 5 ALE3D axisymmetric wedge mesh for cookoff of Comp B in STEX Test TE-012.

After a temperature reaches a user-specified threshold value, the multi-step kinetics model is replaced by the burn front expression (4). The burn front is propagated through the HE with the assumption that reactants are converted completely to products in a single step. This burn front is tracked using a level set method that conserves mass, momentum, and energy across the front. Since the mesh is not moved to explicitly track the front, the resolution of the burn front is on the scale of the mesh element size. The effects of mesh size are an important consideration under current investigation.

COMPARISON OF MODEL AND MEASURED THERMAL COOKOFF RESULTS

In cookoff Test TE-012 for Comp B, the set-point temperature for TC1 was increased in stages from room temperature to 130°C, held for 5.0 h, and then increased at 1°C/h until cookoff[10] (see Figures 1 and 6). The measured center internal temperature TC6 shows a dip around 80°C which is probably related to the melting of TNT. After the hold at 130°C, the top and bottom set-point temperatures TC2 and TC3 are kept 9°C and 4°C cooler than TC1, respectively. The calculated cookoff temperature of 162°C (T1) compares favorably with the measured value of 160°C (see Figure 6).

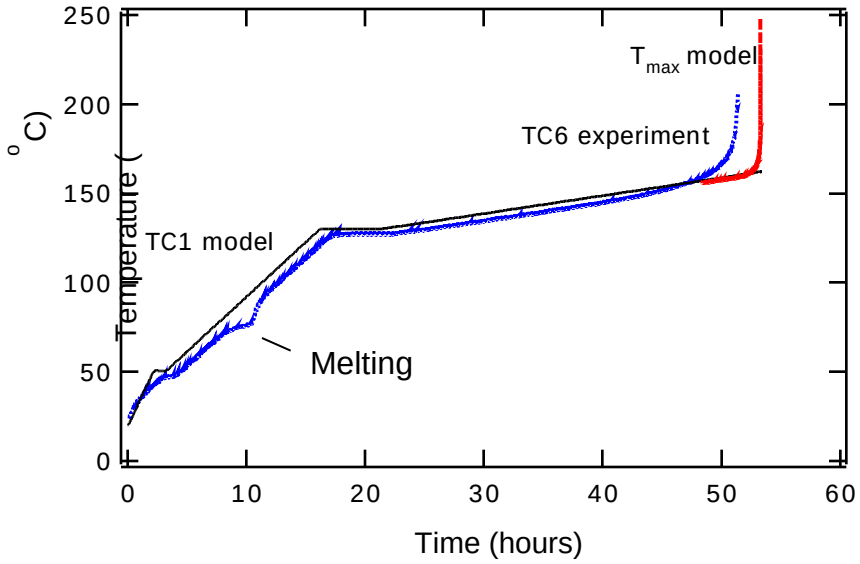

Figure 6 Comparison of measured and model temperatures for Comp B STEX test.

The measured internal temperature TC6 begins to rise relative to the wall temperature TC1 approximately 6 h before ignition as a result of heat released from decomposition. The maximum model temperature, T_{max}, increases later, but more rapidly. The last measured value of 208°C is above the RDX melting point of 205°C resulting in an all fluid hot zone. This fluid hot zone is also seen in both measured and calculated temperature fields at ignition (see Figure 7). The liquid and gas chemical species are quite mobile and and move as result of buoyancy effects. Density gradients are generated by variations in temperature and composition which results in the flow of hot liquid and gases towards the top of the vessel. Note that this type of flow also occurs elsewhere in the system as liquid TNT and product gases percolate through a matrix of solid RDX. The much higher measured temperatures in the upper portion of the vessel are evidence for these free convection effects. It is seen that the all fluid zone extends well up into the upper portion of the vessel and the top thermocouple temperature TC4 in the HE is 9°C above the upper control temperature TC2. The current model does not include free convection effects, and the model reaction energy is confined to a much smaller region near the ignition point. These buoyancy effects may lead to increased mixing of material and energy and change the conditions at ignition.

A large amount of violence was seen in this test with Comp B (see Figure 8). A large number of fragments were formed and holes were punched through the end caps. Radar velocity measurements showed fragment velocities of 2000 m/s and the release of approximately 100% of the energy based on a Gurney energy calculation [6].

Calculated density fields show the filling of the air gaps, the formation of HE product gases, and the expansion of the tube wall (see Figure 9). The high burn rate model (No. 2) is used in these calculations. Initially, the air gap occupies the top 8% of the vessel volume. About 5.3 h before ignition, the air gap is nearly filled by the HE and the tube wall does not show obvious expansion. At t=29 μs, the product gas is evident and the burn front is advancing. The wall velocity is 350 m/s at this time. At t=124 μs, the wall has expanded dramatically over the entire length of the tube, and a sizeable fraction of the

HE has burned. Since the model Comp B has no strength, the pressure increase resulting from the deflagration is distributed over the length of the tube. As a result the contour of the expanded tube is very smooth. It is noted that the tube is likely to have fragmented by this time. The wall velocity is 390 m/s indicating a modest acceleration relative to the results at t=29 μs. For comparison, radar measurements of fragment velocities in this test gave an average value of 2000 m/s, a far larger value. Differences in these values may in part be related to the absence of fragment formation in the model.

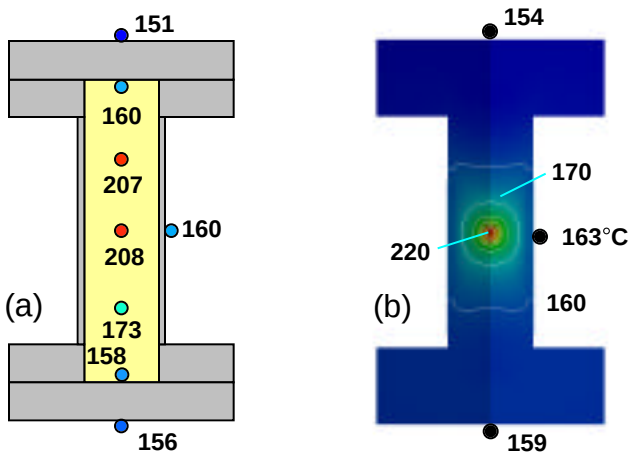

Figure 7 Measured (a) and model (b) temperature contours for ALE3D model for a STEX test with Comp B. Contours increase from 160 ^{o}C to 220^{o}C in 10^{o}C increments for the model results.

Figure 8 Fragments from STEX Test No.TE-012 for Comp B.

For the slow heating phase, the ALE3D model strain curve is compared with the measured curves for the hoop strain gauges SG1 and SG2 at the axial midplane (see Figure 10). The gauges SG1 and SG2 have measurement limits of 8 and 2% strain, respectively. Also shown is a theoretical strain curve for the expansion of an empty steel vessel calculated from the steel CTE and the TC1 set-point temperature. The measured results for SG1 and SG2 follow the empty vessel curve until the final pressurization. This is an expected result since, since the Comp B material with liquid TNT has little strength and should expand freely until either the gap is filled or decomposition gases pressurize the vessel. There are slight differences between the two measurement curves due to different treatments of the contribution of steel expansion. For SG1, the thermal expansion of steel was added after the test whereas for SG2 the effects of steel were included as part of the measurement.

As expected, the model results oscillate about the empty vessel results until ignition takes place. The amplitudes for the oscillations are large on the scale of the steel strain, showing the effects of the

artificial density needed to carry out the mechanical calculations explicitly. The period of the oscillations ranges from 1 to 3 h which is a time scale judged to be acceptable for these calculations. Pressure waves propagate in the axial direction through the no-strength Comp B mixture as a result of the mass scaling and changes in thermal conditions. Pressures are generally of the scale 100 bar (10 MPa) with some transients as large as 1 kbar (100 MPa) until the final hours before ignition. We plan to explore adjustments in the artificial viscosity to provide increased damping of these mechanical results. In addition, implicit methods are being developed for these cases with soft materials and gaps. Nonetheless, these are the most accurate mass scaling calculations carried out to date for slow cookoff. We believe that it is important to have accurate mechanical results at the time of ignition, since the subsequent deflagration is strongly dependent on the pressure in the ignition area.

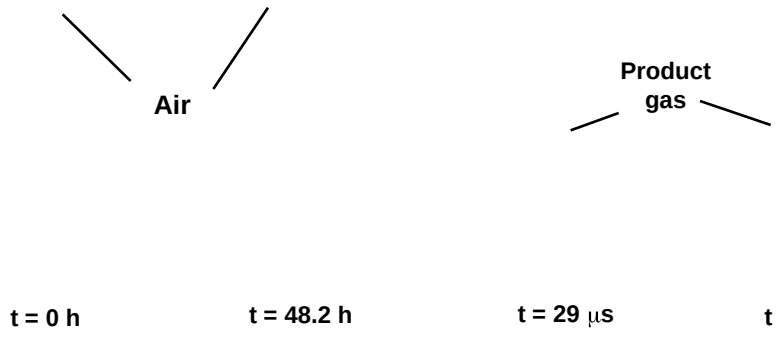

Figure 9 ALE3D density fields for ALE3D model of Comp B heating and deflagration. Times for the last two frames are measured from the start of the rapid expansion.

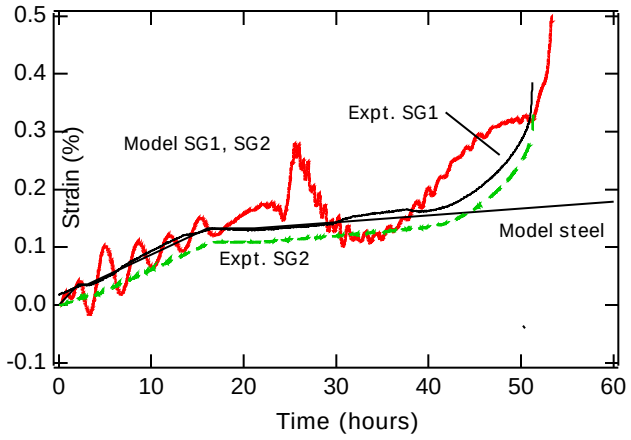

Figure 10 Comparison of ALE3D strains with measurements for STEX test with Comp B during the heating phase.

Experimental and model hoop strain results for the rapid expansion are shown in Figure 11. The time scale for the measured results for SG1 is 2500 μs, a relatively long time for an expansion to an 8% strain. Note that the 8% strain is the measurement limit of this gauge. The wall velocity based on these measurement is only 3 m/s at 8% strain. The wall is strongly accelerated after this point to reach the measured fragment velocities of 2000 m/s. Such low strain rates were observed in other STEX tests with Comp B, confirming that these results are reproducible. The expansions for Model nos. 1 and 2 have much shorter time scales of 210 and 40 μs, respectively, for the 8% expansion. Model no.1 uses the lower bound for the measured burn rates, and Model no. 2 passes through the middle of the data (see Figure 3). Some of the irregularities in the model curves are believed to be the result of inadequate mesh resolution. Although the reasons for the poor agreement are not known at this time, we suspect they are

related to free convection of liquid and gas prior to the burn and the complex burn behavior of Comp B. There are questions concerning the scatter in the data, and the behavior at pressures above 120 MPa (1.2 kbar), the upper limit for the strand burner measurements. At the onset of burning, calculated burn rates are as high as 10 kbar (1 GPa), and the question remains as to burn behavior at these conditions.

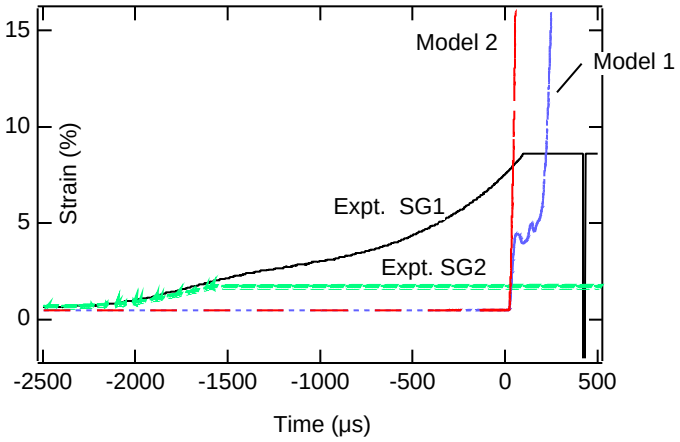

Figure 11 Comparison of ALE3D strains with measurements for STEX test with Comp B during the explosive phase.

CONCLUSIONS

A STEX cookoff test is analyzed using the ALE3D computer code which incorporates models for thermal, mechanical, and chemical behavior. In this test, a Comp B sample with L/D~4 is heated slowly in a sealed tube until explosion. The ALE3D code is used to simulate thermal, mechanical, and chemical behavior on the long time scales of heating and short time scales of explosion. Tarver-McGuire models are selected to represent the chemical kinetics of the RDX and TNT behavior during heating. A power-law burn rate model is employed during the rapid expansion phase. Parameters for the Tarver-McGuire models were specified using ODTX measurements, and two sets of power-law parameters were selected to represent strand burner measurements. These burn rate measurements show considerable scatter, which is possibly associated with deconsolidation. A Steinberg-Guinan mechanical model and polynomial EOS are selected for the RDX and TNT solid species. Since TNT is a liquid at the temperatures of cookoff, the mixture is assumed to have no strength in both the slow heating and rapid expansion. A Gamma-Law model is used for the product gases and air in gaps.

Cookoff simulations for a two-dimensional axi-symmetric model were completed for the thermal ramp, ignition, and rapid expansion of the tube. For the test considered, the predicted cookoff temperature is in good agreement with the measured value, but the measured temperature fields show the effects of buoyancy-driven convection not seen in the calculations. The model provides an approximate representation of strains measured during the slow heating, but does not yet provide a good description of the surprisingly small measured strain rates seen during the early stages of the explosion.

REFERENCES

1. Wardell, J. F. and J. L. Maienschein, "The Scaled Thermal Explosion Experiment," Proceedings of 12th Internation Detonation Symposium, San Diego, CA, 2002.

2. Maienschein, J. L., J. F. Wardell, R. K. Weese, B. J. Cunningham and T. D. Tran, "Understanding and Predicting the Thermal Explosion Violence of HMX-Based and RDX-Based Explosives - Experimental Measurements of Material Properties and Reaction Violence," Proceedings of 12th International Detonation Symposium, San Diego, CA, 2002.

3. Kaneshige, M. J., A. M. Renlund, R. G. Schmitt and W. W. Erikson, "Cook-Off Experiments for Model Validation," Proceedings of JANNAF 38th Combustion and 20th Propulsion Systems Hazards Subcommittee Meetings, Destin, Fl, 2002.

4. Sandusky, H. W. and G. P. Chambers, "Validation Experiments for Slow Cookoff," Proceedings of JANNAF 38th Combustion and 20th Propulsion Systems Hazards Subcommittee Meetings, Destin, Fl, 2002.

5. Nichols, A. L., A. Anderson, R. Neely and B. Wallin, "A Model for High Explosive Cookoff," Proceedings of 12th Internation Detonation Symposium, San Diego, CA, 2002.

6. McClelland, M. A., J. L. Maienschein, A. L. Nichols, J. F. Wardell, A. I. Atwood and P. O. Curran, "ALE3D Model Predictions and Materials Characterization for the Cookoff Response of PBXN-109," Proceedings of JANNAF 38th Combustion and 20th Propulsion Systems Hazards Subcommittee Meetings, Destin, Fl, 2002.

7. Erikson, W. W. and R. G. Schmitt, "Pre- and Post-Ignition Modeling of Validation Cookoff Experiments," Proceedings of JANNAF 38th Combustion and 20th Propulsion Systems Hazards Subcommittee Meetings, Destin, Fl, 2002.

8. Atwood, A. I., P. O. Curran, D. M. Hanson-Parr, T. P. Parr and D. A. Ciaramitaro, "Experimental Input Parameters Required for Modeling the Response of PBXN-109 to Cookoff," Proceedings of JANNAF 37th Combustion and 19th Propulsion Systems Hazards Subcommittee Meetings, Monterey, CA, CPIA, 2000.

9. Erikson, W. W., R. G. Schmitt, A. I. Atwood and P. O. Curran, "Coupled Thermal-Chemical-Mechanical Modeling of Validation Cookoff Experiments," Proceedings of JANNAF 37th Combustion and 19th Propulsion Systems Hazards Subcommittee Meetings, Monterey, CA, 2000.

10. Atwood, A. I., P. O. Curran, M. W. Decker and T. L. Boggs, "Experiments for Cookoff Model Validation," Proceedings of JANNAF 37th Combustion and 19th Propulsion Systems Hazards Subcommittee Meetings, Monterey, CA, CPIA, 2000.

11. Atwood, A. I., P. O. Curran, K. B. Lee and D. T. Bui, "Experimental Progress on a Cookoff Model Validation Effort," Proceedings of JANNAF 38th Combustion and 20th Propulsion Systems Hazards Subcommittee Meetings, Destin, Fl, 2002.

12. McClelland, M. A., T. D. Tran, B. J. Cunningham, R. K. Weese and J. L. Maienschein, "Cookoff Response of PBXN-109: Material Characterization and ALE3D Model," Proceedings of JANNAF 37th Combustion and 19th Propulsion Systems Hazards Subcommittee Meetings, Monterey, CA, CPIA, 2000.

13. McClelland, M. A., T. D. Tran, B. J. Cunningham, R. K. Weese and J. L. Maienschein, "Cookoff Response of PBXN-109: Material Characterization and ALE3D Thermal Predictions," Proceedings of 50th JANNAF Propulsion Meeting, Salt Lake City, UT, CPIA, 2001.

14. Yoh, J. J. and M. A. McClelland, "Simulating the Thermal Response of High Explosives on Time Scales of Days to Microseconds," Proceedings of 13th American Physical Society Topical Conference on Shock Compression of Condensed Matter, Portland, OR, 2003.

15. McClelland, M. A., J. L. Maienschein and A. L. Nichols, "Joint DoD/DOE Munitions Technology Development Program FY-01 Progress Report, Ignition and Initiation Phenomena: Cookoff Violence Prediction," Lawrence Livermore National Laboratory, 2002.

16. McClelland, M. A., J. L. Maienschein, A. L. Nichols and J. J. Yoh, "Joint DoD/DOE Munitions Technology Development Program FY-02 Progress Report, Ignition and Initiation Phenomena: Cookoff Violence Prediction," Lawrence Livermore National Laboratory, 2003.

17. McGuire, R. R. and C. M. Tarver, "Chemical Decomposition Models for the Thermal Explosion of Confined HMX, TATB, RDX,and TNT Explosives," Proceedings of Seventh Symposium (International) on Detonation, Annapolis, MD, Naval Surface Weapons Center, 1981.

18. Tran, T. D., R. L. Simpson, J. L. Maienschein and C. M. Tarver, "Thermal Decomposition of Trinitrotoluene (TNT) with a New One-dimensional Time to Explosion Apparatus," Lawrence Livermore National Laboratory, UCRL JC-141597, 2000.

19. Nichols, A. L. and K. W. Westerberg, "Modification of a Thermal Transport to Include Chemistry with Thermally Controlled Kinetics," ***Numerical Heat Transfer, Part B***, vol. 24, pp. 489-503, 1993.

20. Steinberg, J., "Equation of State and Strength Properties of Selected Materials," Lawrence Livermore National Laboratories, UCRL-MA-106439, Livermore, CA, 1996.

21. Fried, L. E., W. M. Howard and P. C. Souers, "Cheetah 2.0 User's Manual," Lawrence Livermore National Laboratories, UCRL-MA-117541 Rev. 5, 1998.

22. Bird, R. B., W. E. Stewart and E. N. Lightfoot, ***Transport Phenomena,*** Wiley, pp. 260-261, 1960.

23. Catalano, E., R. McGuire, E. L. Lee, E. Wrenn, D. Ornellas and J. Walton, "The Thermal Decomposition and Reaction of Confined Explosives," Proceedings of Sixth International Symposium on Detonation, Coronado, CA, Office of Naval Research, 1976.

24. Shapiro, A. B. and E. A. L, "TOPAZ2D Heat Transfer Code Users Manual and Thermal Property Data Base," Lawrence Livermore National Laboratory, UCRL-ID-104558, 1990.

25. Cooper, P. W., ***Explosives Engineering,*** Wiley-VCH, pp. 258, 1996.

26. Morari, M. and E. Zafiriou, ***Robust Process Control,*** Prentice Hall, pp. 116-117, 1989.

27. Holman, J. P., ***Heat Transfer,*** McGraw-Hill, pp. 253-254, 1976.

28. Sharp, R., "Users Manual for ALE3D An Arbitrary Lagrange/Eulerian 3D Code System," Lawrence Livermore National Laboratory, 2003.